

# 1 FUNDAMENTALS

## 1.1 MEANING OF ISOSTASY AND RIGIDITY

Isostasy is a term derived from the Greek words “iso” and “stasis” meaning “equal standing”. The term is used to describe an equilibrium to which the Earth’s crust and mantle tend, in the absence of disturbing forces (WATTS 2001). Some of the first ideas about the equilibrium of the Earth’s outer layers originate from the engineer, artist and humanitarian, LEONARDO DA VINCI (1452-1519). Translation of da Vinci’s notebooks by MACCURDY (1956) shows that he had given considerable thought how the Earth might respond to shifts in loads over its surface.

It was just 200 years later, when the first attempts were made to determine the shape of the earth, that it was possible to estimate the equilibrium state of mountains. The concept of isostasy was discovered during the late 1880’s as part of a geodetic survey of northern India, and describes the compensation of topographic masses by the restoring force of the mantle. But the depth of compensation and the restoring force are in a different way described and mathematically understood. There are 2 classical contrary schemes from PRATT (1855) and AIRY (1855) distinguished. Both schemes are based on the idea of local compensation of the topographic masses. By the 1930s, two schools of thought had emerged: an American school, which favored the Pratt model, and a European one that preferred the Airy model. During the 1940s/1950s the predictions of the two models had begun to be compared with observations on the seismic structure of oceanic and continental crust and the underlying mantle. But to many scientists these models were inconsistent with the known geological facts, ignoring as they did the strength of the crust and upper mantle.

The idea that loads on the Earth’s surface may be regionally rather than locally supported can be traced back to the work of BARRELL (1914). He challenged the conclusion of the geodesists concerning local models of isostasy, invoking instead the idea that topography was supported regionally by the lateral strength of the lithosphere (BARRELL 1914). At present, the best-known model is the Vening-Meinesz model.

### 1.1.1 Isostasy according to Pratt

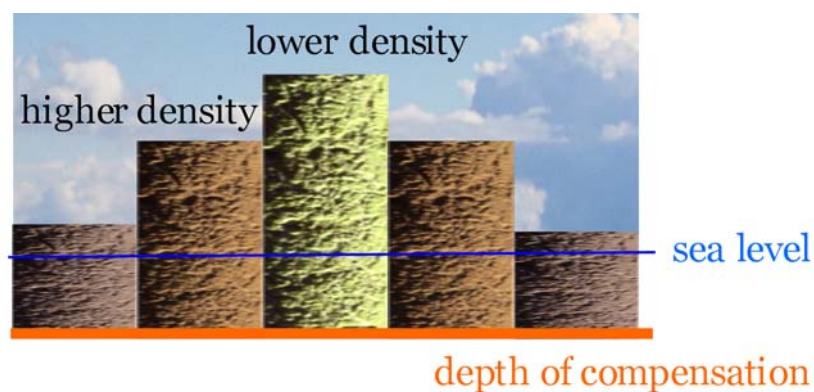


**Figure 1.1.1)** The isostasy according to Pratt is a model of local compensation with variation of densities and constant depth of compensation.

The isostatic model after PRATT (1855) is based on the idea that the restoring forces of local compensation are caused by lateral density variation in the underground (Fig. 1.1.1). It is assumed that topographic masses are compensated at a constant depth, hence it follows that the densities within the crust are changing. This for example means that in mountain belts the crustal density is less than in flat areas. Today this model is still used for passive continental margins, but in case of areas with higher topography the approach contradicts e.g. seismic observations.

### 1.1.2 Isostasy according to Airy

The model according to AIRY (1855) is also known as Airy-Heiskanen approach. Airy's argument was based on his belief that the outer layers of the Earth consisted of a thin crust that overlay a layer of greater density than the crust (Fig. 1.1.2).

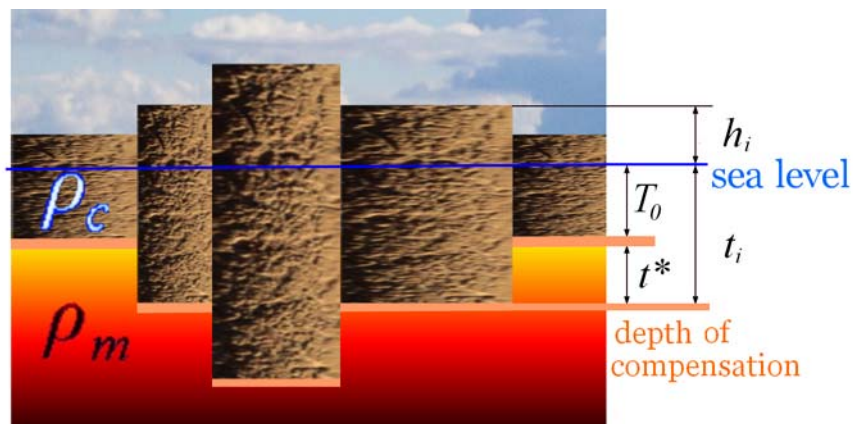


**Figure 1.1.2)** Model with variation of the depth of compensation and Description for formula of Airy compensation for the root and densities.

Airy compared the state of the crust lying on lava to timber blocks floating on water. In this model the depth of compensation is not constant. However, the density of the crust is constant, which leads to a variability of the depth of compensation. This idea based on the concept of static equilibrium. For  $\forall i = 1, \dots, n$  with  $n \in \mathbb{N}$  the depth  $t_i$  follows directly from the topographic heights  $h_i$  (see Fig. 1.1.2). With  $t^*$  as the crustal root,  $T_0$  as normal crustal thickness (e.g.  $T_0 = 35\text{km}$ ),  $\rho_c$  as the density of the crust and  $\rho_m$  as density of the mantle the following equation can be derived:

$$t_i(x, y) = -T_0 - \underbrace{\frac{\rho_c}{\rho_m - \rho_c}}_{t^*} h_i(x, y) \quad (1.1.1)$$

### 1.1.3 Isostasy according to Vening-Meinesz

The calculation and estimation of the isostasy according to VENING-MEINESZ (1939) is principally based on the Airy-model. Vening-Meinesz introduced a new method for the reduction of gravity data. He assumed that the compensation of the earth's surface features was not necessary local, instead might be regional. He regarded topography as a load on the surface of the crust. In this view, the load causes the crust to bend, producing a low-density

root similar to that predicted by the Airy model. The main difference with the Airy model, however, was that the root would be broader because the load is now supported, at least in part, by the rigidity of the crust. The thin plate flexure model according to BANKS ET AL. (1977) involves regional isostatic compensation, and opposed the older models of local compensation of PRATT and AIRY. It has been evolved from the isostatic model of VENING-MEINESZ.

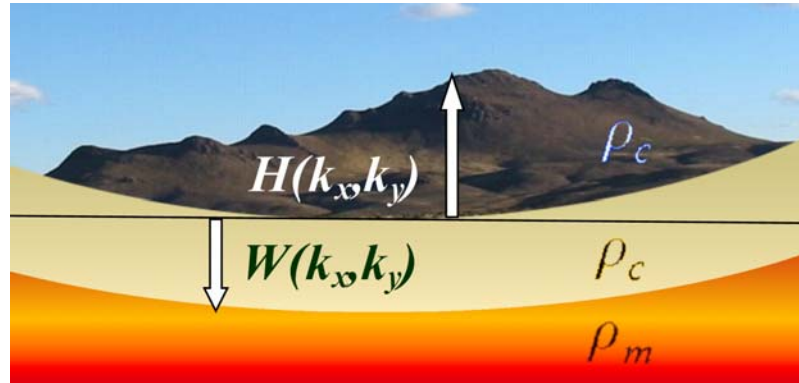


**Figure 1.1.3)** If no load is acting, then the bottom of the plate can be described with a horizontal line in the  $x-z$  or  $y-z$  direction. The deflection from this horizontal line is denoted with  $w$  or  $W(k_x, k_y)$ , respectively.

For a homogeneous isotropic elastic plate, the problem has been transformed in the frequency space (see Chapter 1.2.1).  $H(k_x, k_y)$  is the Fourier transform of the topography  $h$  and  $W(k_x, k_y)$  is the Fourier transform of the flexure  $w$  (Fig. 1.1.3). The flexure  $W(k_x, k_y)$  of the plate is related to the topography  $H(k_x, k_y)$  with:

$$W(k_x, k_y) = \frac{1}{\frac{\rho_m}{\rho_c} - 1 + \frac{D}{g\rho_c} \left[ (k_x, k_y) \right]^4} \cdot H(k_x, k_y) \quad (1.1.2)$$

If no load is acting then the plate remains flat and the bottom of the plate can be described in two dimensions as an horizontal line. The deflection from this horizontal line caused by a load is called flexure  $w = w(x, y)$ . Like in the equation above  $\rho_c, \rho_m$  are the crust and mantle densities,  $g$  is the normal gravity,  $\vec{k}$  is the two dimensional wavenumber, and  $D$  the flexural rigidity of the plate. If the flexural rigidity goes to zero then the equation 1.1.2 leads to equation 1.1.1 for the local compensation according to Airy in the space domain. The Fourier transform  $W(k_x, k_y)$  corresponds to the crustal root  $t^*$ , the Fourier transform  $H(k_x, k_y)$  corresponds to the topographic heights  $h_i$ , and the wave numbers  $k_x, k_y$  corresponds to the Cartesian coordinates. This is mathematically the same description for the fact that plates without strength collapse in local isostasy (see Chapter 1.1.4).

### 1.1.4 Elastic thickness and flexural rigidity

Vening-Meinesz introduced the concept that the flexural strength of the lithosphere had to be taken into account in isostatic consideration. The parameter that characterizes the apparent flexural strength of the lithosphere is the flexural rigidity  $D$ , which is commonly expressed through the elastic thickness  $T_e$  of the lithosphere. The flexural rigidity of the plate  $D$  is defined in terms of Young's modulus  $E$ , the Poisson's ratio  $\nu$  and the elastic thickness  $T_e$  with the following equation:

$$D = \frac{E \cdot T_e^3}{12(1 - \nu^2)} \quad (1.1.3)$$

If one refers to the elastic thickness instead of the flexural rigidity, one implies a choice of rheological model. Thereby standard values are used with  $E = 10^{11} Pa = 10^{11} Nm$  and  $\nu = 0.25$ .

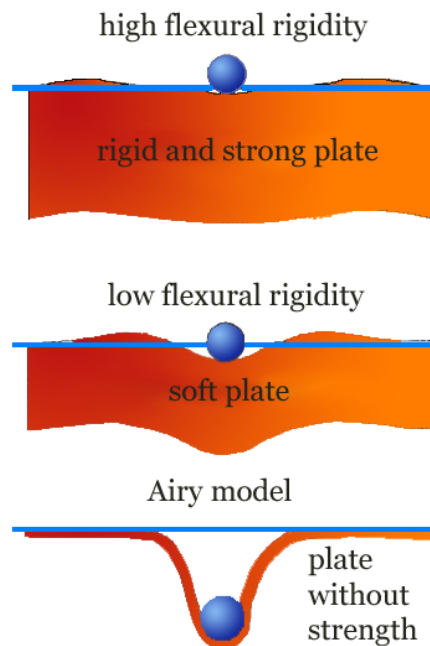


**Figure.1.1.4)** The elastic behavior of plates change for different rigidities. Plates without rigidity are collapse in a local isostasy according to Airy.

The deflection of the plate depends on the properties of the plate, or in other words: how resistant is the material of the plate against a deformation. The classical Airy model for local compensation corresponds to a flexural model where the plate has no strength; this means an elastic thickness value of zero (Fig. 1.1.4). For this reason, in Chapter 2, where the analytical solution is developed, it is important that this solution converges to the solution according to Airy, if the value for the elastic thickness converges to zero (see Chapter 2.5). In the past usually the calculation was done in the frequency space with fast Fourier transformation techniques (short: FFT), which are investigated in the following Chapter 1.2.

## 1.2 METHODS FOR ESTIMATION OF FLEXURAL PARAMETERS

In general, all models on the mechanical behavior of the lithosphere consider the lithosphere as a closed system with a black box response to external parameters: the input variables include surface and subsurface loads, density variations, forces and bending moments, whereas the output variables consist of the geometry of the substratum, deflections of the CMI and gravity anomalies (e.g. FORSYTH 1980, McNUTT 1980, LYON-CAEN & MOLNAR 1983, BUROV & DIAMENT 1995, KÖSTERS 1999, BRAITENBERG 2001). Irrespective of the real strain and stress distribution occurring within the deformed lithosphere, one can always estimate an “equivalent” or “effective” elastic plate thickness that will relate the output to the input by matching the observed deflection of the plate to the calculated deflection.

The calculations of the elastic thickness provided a convenient basis for the comparison of continental regions (McNUTT ET AL. 1988, EBINGER ET AL. 1989, BECHTEL ET AL. 1990). However, no information on the internal structures of the lithosphere was used in these investigations and the assumed mechanical properties of the plate only parameterized the “response function” of the lithosphere and therefore, it was not possible to provide any insights into the actual “black box”.

### 1.2.1 Spectral methods

In the 1970’s spectral techniques have been developed to better quantify the degree of isostatic compensation. The relationship between gravity and topography over a surface load changes as a function of wavelength.

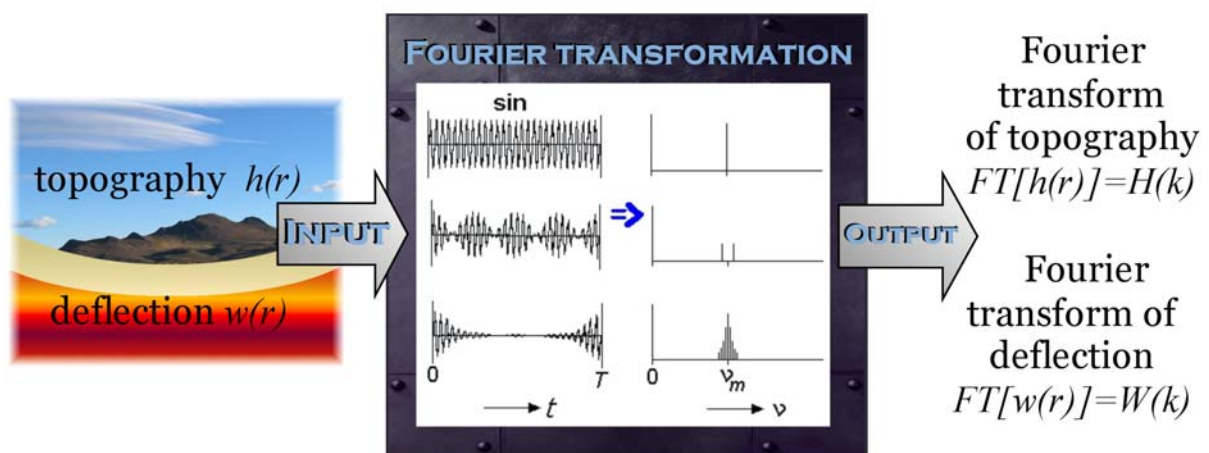


**Figure 1.2.1)** To describe the Fourier transformation in a simple way the transformation is illustrated as black box, as an example the sine function is given. On the left side the space domain is shown and on the right side the frequency or wave number domain. If I consider e.g. a function that can be described as a sum of 3 various sine functions, then this function corresponds to 3 peaks in the frequency domain. Hence, the topography and the deflection can be described as functions of wavelength, and therefore be transferred into the frequency domain, where the computation is simpler.

Therefore, by analyzing the frequency of observed gravity and topography data over a feature and comparing the spectra with the prediction of both local and regional models of isostasy it

has been possible to determine the compensation scheme. A widely used technique to decompose a spatial data set into its spectral components is the Fourier analysis. In Figure 1.2.1 the Fourier transformation is described in a simple example. According to Fourier's law, every wave function can be decomposed as a sum of sine and cosine functions. Accordingly, the topography and the CMI undulation can be transferred into a wave function, and therefore into the frequency domain where the computation is simpler. For example a sine function corresponds to a single peak in the wavenumber domain. In order to multiply two functions in the space domain, it is necessary to use the convolution; but in the wavenumber domain, this can be done by a simple multiplication. Accordingly, the spatial variation in flexure due to a 2 dimensional load is obtained by first taking the Fourier transform of the load, multiplying it by a wavenumber parameter and a density term, and then inverse transforming it (see Chapter 2.4, Fig. 2.4.1).

With the approach by PARKER (1972) it became possible to relate the Fourier transform of the gravity anomaly  $FT[\Delta g_p(\vec{r})]$  at a point  $P$  and  $FT[\Delta g_Q(\vec{r})]$  at a point  $Q$  with a distance  $d$ . From the potential theory follows in the first order:

$$FT[\Delta g_p(\vec{r})] = e^{-|\vec{k}|d} FT[\Delta g_Q(\vec{r})] \quad (1.2.1)$$

with  $\vec{r} = r(x, y)$  as two dimensional vector in the space domain and  $(\vec{k}) = k(k_x, k_y)$  as wavenumber in the frequency domain. This approach by Parker will be used in the next chapter (see Chapter 1.3). The gravity anomaly  $FT[\Delta g_p(\vec{r})]$  can be replaced by an equivalent surface mass distribution  $M_Q[\vec{k}]$  on the same plane that is given by:

$$M_Q[\vec{k}] = \frac{FT[\Delta g_Q(\vec{r})]}{2\pi G} \quad (1.2.2)$$

If  $M_Q[\vec{k}]$  is a surface mass, it follows:

$$FT[\Delta g_Q(\vec{r})] = 2\pi G(\Delta\rho)W(\vec{k}) \quad (1.2.3)$$

$W(\vec{k})$  is the Fourier transform of the surface of an undulating interface and  $\Delta\rho$  is its uniform density contrast. If I put Eq. 1.2.1 into Eq. 1.2.3, I obtain:

$$FT[\Delta g_p(\vec{r})] = 2\pi G(\Delta\rho)e^{-|\vec{k}|d} W(\vec{k}) \quad (1.2.4)$$

An important parameter that modifies the topography so as to produce the gravity anomaly is the gravitational admittance  $Z(\vec{k})$ . This wavenumber parameter contains information about the degree of isostasy and is given by:

$$Z(\vec{k}) = \frac{\text{input}}{\text{output}} = \frac{FT[\Delta g(\vec{r})]}{W(\vec{k})} \quad (1.2.5)$$

### Isostatic response function

When discussing a gravity anomaly (WATTS 2001), it is very useful to utilize a wavenumber parameter that modifies the gravity effect of the topography so as to produce the gravity anomaly. The wavenumber parameter  $\varphi_e(\vec{k})$  that describes the behavior of such a system is given by:

$$\varphi_e(\vec{k}) = \frac{\text{output}}{\text{input}} \quad (1.2.6)$$

From Eq. 1.2.4 follows for the density contrast  $\rho_c - \rho_w = \Delta\rho$  and the 2 dimensional wavenumber  $(\vec{k}) = (k_x, k_y)$ :

$$\text{input} = 2\pi G e^{-\vec{k}d} (\rho_c - \rho_w) \cdot H(\vec{k}) \quad (1.2.7)$$

$H(\vec{k})$  is the Fourier transform of the surface of an undulating interface, which corresponds in this case to the topography. For the Airy model results:

$$\text{output} = 2\pi G e^{-\vec{k}d} (\rho_c - \rho_w) \cdot H(\vec{k}) \cdot (1 - e^{-\vec{k}t}) \quad (1.2.8)$$

it follows:  $\Rightarrow \varphi_e(\vec{k})_{\text{airy}} = (1 - e^{-\vec{k}t}) \quad (1.2.9)$

In the case of the flexure model (in its simplest form):

$$\text{output} = 2\pi G e^{-\vec{k}d} (\rho_c - \rho_w) \cdot H(\vec{k}) \cdot (1 - \Phi'_e(k) e^{-\vec{k}t}) \quad (1.2.10)$$

therefore:  $\Rightarrow \varphi_e(\vec{k})_{\text{flexure}} = (1 - \Phi'_e \cdot e^{-\vec{k}t}) \quad (1.2.11a)$

with:  $\Phi'_e(\vec{k}) = \left[ \frac{D\vec{k}^4}{(\rho_m - \rho_c)g} + 1 \right]^{-1} \quad (1.2.11b)$

It is seen from the equations (1.2.11a-b) that  $\varphi_e(\vec{k})_{\text{flexure}}$  is independent of the mean water depth and the density difference between crust and seawater. The parameter depends on the thickness of the crust in the Airy model and the flexural properties of the lithosphere in the flexure model (see more in Chapter 2.4). Hence, it provides "direct" information on the state of isostasy for a geological feature and for this reason it is called "isostatic response function".

An advantage of the spectral approach is that statistical methods can be used to estimate  $Z(\vec{k})$  and  $\varphi_e(\vec{k})$  directly from observations. By comparing the "observed" values for these parameters with calculations based on different isostatic models, it should be possible to constrain the state of isostasy. It is seen from Eq. 1.2.4 - 1.2.8:

$$Z(\vec{k}) = \frac{FT(\Delta g(\vec{r}))}{FT(h(\vec{r}))} = \frac{\Delta\Gamma(\vec{k})}{H(\vec{k})} \quad (1.2.12)$$

$$\varphi_e(\vec{k}) = \frac{\Delta\Gamma(\vec{k})}{2\pi G e^{-\vec{k}d} (\rho_c - \rho_w) \cdot H(\vec{k})} \quad (1.2.13)$$

Theoretically, it should be easy to determine  $Z(\vec{k})$  by dividing the Fourier transform of the observed free-air gravity anomaly  $\Delta\Gamma(\vec{k})$  by the Fourier transform of the topography  $H(\vec{k})$ . The only additional parameters required to compute  $\varphi_e(\vec{k})$  are the mean water depth  $d$  and the density difference between the topography and seawater  $(\rho_c - \rho_w)$ . However, the practical use is difficult, because both data sets need to be transformed. Due to the fact of noise, this could produce spectral estimates with a considerable scatter.

### Oceans

The first applications of spectral techniques in the oceans have been done by MCKENZIE & BOWIN (1976) in the Atlantic and WATTS (1978) in the Pacific. A common approach to estimate the admittance  $Z(\vec{k})$  between two time-series is to divide the Fourier transform of the output function by the transform of the input function.

MCKENZIE & BOWIN (1976) used cross-spectral techniques to estimate  $Z(\vec{k})$  from the free-air gravity anomaly and topography measured along ship tracks. The complex admittance for a particular wavenumber is given by:

$$Z(\vec{k}) = \frac{C_s(\vec{k})}{P_t(\vec{k})} \quad (1.2.14)$$

where  $C_s(\vec{k})$  is the cross-spectrum of the gravity anomaly and topography and  $P_t(\vec{k})$  is the power spectrum of the topography  $C_s(\vec{k})$  and  $P_t(\vec{k})$  are given by:

$$C_s(\vec{k}) = \frac{1}{N} \sum_{m=1}^N \Delta\Gamma_m(\vec{k}) H_m^*(\vec{k}) \quad (1.2.15)$$

and

$$P_t(\vec{k}) = \frac{1}{N} \sum_{m=1}^N H_m(\vec{k}) H_m^*(\vec{k}) \quad (1.2.16)$$



The asterisk \* denotes the complex conjugate, and  $\Delta\Gamma_m(k)$  and  $H(\vec{k})$  are the discrete Fourier transforms of the observed free-air gravity anomaly and topography, respectively. The methodology of MCKENZIE & BOWIN (1976) and WATTS (1978) was similar. Supplementary, they found it useful to compute an additional spectral parameter: the coherence  $\gamma^2(\vec{k})$ . This spectral parameter is calculated by

$$\gamma^2(\vec{k}) = \frac{C_s(\vec{k})C_s^*(\vec{k})}{P_g(\vec{k})P_t(\vec{k})} \quad (1.2.17)$$

whereby:

$$P_g(\vec{k}) = \frac{1}{N} \sum_{m=1}^N \Delta\Gamma_m(\vec{k})\Delta\Gamma_m^*(\vec{k}) \quad (1.2.18)$$

is the power spectrum of the gravity anomaly. The number  $N$  is either the number along-track segments or the number of profiles of the same geological feature.

The success of the early studies lead to an increase in applications of the spectral technique. All these studies were one or two-dimensional, because the problem with three-dimensional spectral studies is that they require closely spaced gravity and topography data over a broad area. This data is difficult to acquire using shipboard surveys. The advantage of high-resolution grids of satellite-derived gravity anomaly data, together with swath bathymetry grids lead to an increased number of three-dimensional spectral studies.

### Continents

Spectral techniques have been applied to continent-wide data sets (e.g. MCNUTT ET AL. 1988, MCKENZIE & FAIRHEAD 1997, KÖSTERS 1999). Unlike oceanic regions, it has been traditional to use the Bouguer rather than the free-air gravity anomaly for the continents. In principle, there should be no difference in the interpretation of spectral data whether free-air or Bouguer anomalies are used.

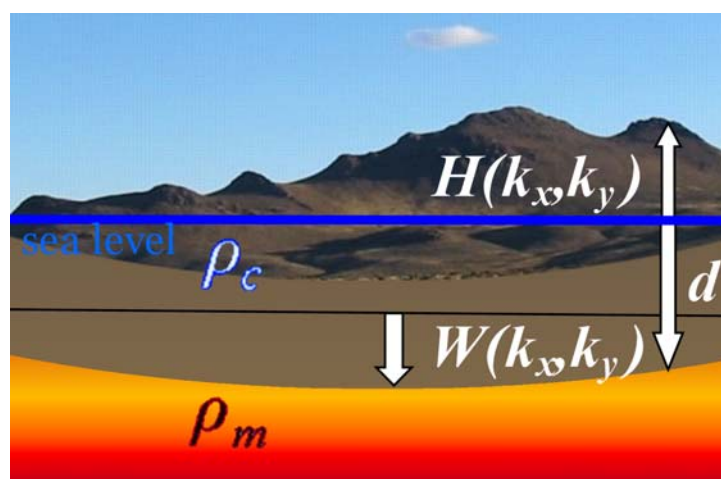


**Figure 1.2.2)** The sketch illustrates a surface-loading model as it applies to the continents, which describes Eq. 1.2.19.

In the case of surface loading, the only contribution to the Bouguer anomaly is from the gravity effect of the compensation:

$$\Delta\Gamma(\vec{k})_{flexure} = 2\pi G(\rho_m - \rho_c) \cdot W(\vec{k}) \cdot e^{-\vec{k}d} \quad (1.2.19)$$

$W(\vec{k})$  is the Fourier transform of the compensation  $w(\vec{r})$  and  $d$  is the depth of the surface of density contrast at the CMI in Fig. 1.2.2 . If the compensation is the consequence of flexure due to a surface load  $H(\vec{k})$ , then it follows from the isostatic response function that:

$$W(\vec{k}) = -\frac{H(\vec{k})\rho_c\Phi_e'(\vec{k})}{(\rho_m - \rho_c)} \quad (1.2.20)$$

for the admittance for the surface loading model it follows:

$$Z(k)_{surface} = -2\pi Ge^{-kd} \rho_c \cdot \Phi_e'(k) \quad (1.2.21)$$

The coherence can be most easily understood by consideration of the "end-member" cases. At short-wavelengths, the coherence approaches zero. This is because the lithosphere appears strong at these wavelengths, independent from its actual  $T_e$  structure. Therefore, the flexure due to a load is small. Conclusively, there will be little contribution from these loads to the Bouguer anomaly. The result is a poor correlation between the Bouguer anomaly and the topography. At long-wavelengths the coherence approaches "1". This is because the lithosphere appears weak at these wavelengths. Surface loads therefore cause a large flexure and so these loads contribute significantly to the Bouguer anomaly. The result is that the Bouguer anomaly will be strongly correlated with the topography. The "roll-over" in the coherence from low to high values therefore reflects the wave-length range for which loads are supported by the finite strength of the lithosphere (WATTS 2001).

KÖSTERS (1999) used the coherence method to calculate the elastic thickness variation, in a part of the Central Andes (see Chapter 3.2) for an area with a side length of  $L = 340km$ , by comparison of the observed coherence with the calculated coherence. (Because the coherence curve was computed for different  $T_e$  values, the best fit to the observed coherence curve provides the associated  $T_e$  value)

### 1.2.2 Advantage and disadvantage of spectral methods

Spectral techniques are a powerful tool for the quantitative examination of the state of isostasy in both, the oceans and continents. For the oceans, the free-air admittance technique has been successful in characterizing the state of isostasy at a wide range of features on the sea-floor, including sea-mounts, oceanic islands, aseismic ridges and mid-oceanic ridges. One reason for this success is that oceanic regions are dominated by surface loading and so there is large contribution to the gravity field of the topography and its compensation. For the continents, the Bouguer coherence technique shows that the continents are characterized by a wide range of  $T_e$  values.

However, for the continents the usefulness of admittance and coherence techniques has been questioned. The drawbacks, which come along with the spectral approach, have been discussed by BRAITENBERG (2001). The first is that it involves an averaging process over the entire grid used for spectral evaluation. In case of a elastic thickness varying in space, the variation may be retrieved only to a limited extent. The limitation is due to the spectral resolution required for the admittance curves. Consequently, a sufficiently large enough spatial window is required. The second problem is due to the fact that the ratio becomes unstable when the spectral values of topography are low, as they are part of the denominator. Additionally, the downward flexed plate was approximated by a series of rectangular prisms of the length  $L$ . Then the error in the gravity calculation of a single prism was determined. BRAITENBERG (2001) concluded that the calculated spectral  $\Gamma_u(\vec{k})$  field is systematically greater than the correct analytical expression  $\Gamma_a(\vec{k})$ . She estimates the relative error with:

$$\frac{\Gamma_u(\vec{k}) - \Gamma_a(\vec{k})}{\Gamma_a(\vec{k})} = \frac{|\vec{k}|L}{1 - e^{-|\vec{k}|L}} - 1 \quad (1.2.22)$$

With an increasing vertical extension (length)  $L$  of the prism the relative error becomes greater. It has been shown that the equation used for the spectral methods is the first term of expansion (according to PARKER 1972) implicating an approximation of the real field. That's why for a downward flexed plate the gravity field will always be overestimated. Another consequence is that the elastic thickness is also overestimated as the observed gravity is interpreted as a less flexed plate than would result from the gravity effect interpretation. The overestimation is more convenient in continental areas, because the crustal root is greater than in oceanic areas. Consequently, different flexure parameters will be obtained (BRAITENBERG ET AL. 2002), whether the admittance of topography/gravity or topography/CMI is calculated.

### 1.2.3 Convolution method

These problems can be overcome by not calculating the flexure parameters with spectral methods, but by the best fit of the observed CMI (e.g. by gravity inversion) and a CMI computed due to a flexure model. The method of gravity inversion and the convolution approach has been extensively tested in synthetic models (BRAITENBERG & ZADRO 1999, BRAITENBERG ET AL. 2002) and in various geographical areas as the Alps (BRAITENBERG ET AL. 1997, ZADRO & BRAITENBERG 1997, EBBING ET AL. 2001) and the Karakorum (BRAITENBERG & DRIGO 1997).

The convolution method works in different steps. The first step is to compute radial symmetric flexure response curves for different elastic thickness values. The impulse response functions were obtained numerically by the Fourier-antitransformation of the filter function on a regular grid using the Vening-Meinesz approach. The second step is to define a radius, which is called the radius of convolution. Outside of the area defined by the radius of convolution the deflection caused by the load is negligible. This method of convolution

developed by BRAITENBERG ET AL. (2002) is applied for each topographic load within this radius of convolution. New ideas about the radius of convolution result from the development of the analytical solution (see Chapter 2.4. and 2.6). The third step is the estimation of the CMI for each elastic thickness (or flexural rigidity, respectively). In a next step the difference of the CMI derived from gravity observations and that obtained due to the flexure is calculated for a window with a side length  $L$ . Varying the elastic thickness minimizes the RMS value of the difference between the two undulating surfaces. If one chooses the minimal RMS value, one can indirectly estimate an elastic thickness for a specific area with side length  $L$ . These steps are illustrated and described in detail in Chapter 2.6.

#### **1.2.4 Advantage and disadvantage of the convolution method**

The only disadvantage of this method is that it requires that the parameters defining the grid of topography have to be chosen carefully, e.g. the distance between the points and number of rows and columns. This is because the choice of the parameters is dictated through the exigency of covering the filter function to sufficiently high frequencies. Additionally, the impulse response should be obtained with a sampling interval comparable to that of the topography grid. This convolution method operates in the space domain and involves the convolution of the topography grid with the flexural response to a point load. The advantage is a higher spatial resolution and a stable result in case of low spectral energy (small topographic heights). This procedure of convolution bears two further advantages: the first is that the analyzed area can be of arbitrary shape, not necessarily square like the condition for the classical spectral methods. The second advantage is that the gravity field is required to be known on a much smaller scale (on the order of  $100km$  length). Only the topography is required to be known over an extensive scale, which depends on the elastic thickness and therefore the radius of convolution. This last condition is much less restrictive with respect to the admittance analysis, where the size of topography and gravity grids must be equal.

#### **1.2.5 Conclusion**

All these approaches for calculating the elastic parameters of the lithosphere are still a closed system, a so-called black box. The calculation remains nontransparent, and there is still a lack of physical understanding. For this reason, I aim to compute the impulse response functions with the new derived analytical solution instead of obtaining the impulse function numerically by the Fourier-antitransformation. This will lead to an adequate answer to the questions about the significance of the convolution radius and other input parameters and the physical meaning of the elastic thickness.

## 1.3 GRAVITY INVERSION ACCORDING TO PARKER ALGORITHM

### 1.3.1 Introduction

The gravity inversion is a useful technique to estimate the Crust-Mantle Interface (CMI) out of the gravity field. This approach will be used for the computation of the flexural rigidity (see Chapter 3.1), because the first part of the work aims modeling the CMI. In this chapter the process of estimation of the CMI by gravity inversion will be introduced. This method requires two input parameter: density contrast and reference depth. The density contrast between crust and mantle is unknown and has to be assumed as a constant value. I will estimate and quantify the errors made because of this assumption. Furthermore the significance of the reference depth will be explained.

The observed gravity field over the earth surface is generated by the 3D density variations in the earth (BRAITENBERG & ZADRO 1999). A complete modeling of the observed gravity field requires a density model that includes variable density in function of depth and position. Thereby the density modeling is feasible only in the case that independent constraining data are available, because according to the theory of potential the problem does not have a unique solution. An approximation to the crustal model can be achieved by reducing the complexity of the density model. Therefore a simple model consists of layers and well-defined density contrasts between the layers. In a simplified crustal model, the gravity field may be explained by the undulations of the surfaces of the layers defined by the major discontinuities in density. Vice versa can the depth variations of the discontinuity be inverted from the gravity data. Due to the  $\frac{1}{r}$  dependence of the gravity potential field, the short wavelength variations of the gravity field are filtered out with increasing distance to the mass source (e.g. ZADRO 1986). It follows that in most cases only the long-wavelength part of the observed gravity field is generated by the CMI, except for long-stretched sedimentary basins. The method of gravity inversion has been extensively tested on synthetic models (BRAITENBERG & ZADRO 1999).

### 1.3.2 Method

This method requires the reference depth  $d$  of the density interface and the density contrast across the interface  $\Delta\rho$  as starting parameters. If  $g_0(x, y)$  is the Bouguer gravity field in Cartesian coordinates  $x, y$  and  $g_d(x, y)$  is the downward continued field to the depth  $d$ , then the Fourier transform of the Bouguer gravity field  $\Gamma_0 = FT[g_0]$  can be related to the Fourier transform of the gravity field  $FT[g_d] = \Gamma_d(k_x, k_y)$  with:

$$FT[g_d] = \Gamma_d(k_x, k_y) = e^{d\xi} \Gamma_0(k_x, k_y) \quad \text{with } \xi = \sqrt{k_x^2 + k_y^2} \quad (1.3.1)$$

thereby are  $k_x, k_y$  the wave numbers along the coordinate axes. It is assumed that the field is generated by a sheet mass located at the depth  $d$ . The surface density of a this mass  $\rho(x, y)$  is given by:

$$\rho(x, y) = \frac{1}{2\pi G} g_d(x, y) = \frac{1}{2\pi G} FT^{-1}[\Gamma_d(k_x, k_y)] \quad (1.3.2)$$

with  $FT^{-1}$  as the inverse Fourier Transform and  $G$  as gravitational constant. The mass that produces the gravity field can be interpreted as a horizontally varying surface density. This can be described with a model of an undulating boundary, which separates two layers with a density contrast  $\Delta\rho$  (BRAITENBERG & ZADRO 1999). The undulation amplitude of the boundary is then given by:

$$r_1(x, y) = \frac{1}{\Delta\rho} \rho(x, y) \quad (1.3.3)$$

Only in first approximation does the gravity field, generated by the vertically expanded boundary, coincide with the field  $g_0(x, y)$  as shown by PARKER (1972). BRAITENBERG & ZADRO (1999) approximate the vertically expanded boundary with a series of rectangular prism and calculate the gravity field  $g_1(x, y)$  by applying the algorithm developed by NAGY (1966). The residual gravity field  $\delta g_1(x, y)$  is defined as the difference between the observed field  $g_0(x, y)$  and the calculated field  $g_1(x, y)$ :

$$\delta g_1(x, y) = g_0 - g_1 \quad (1.3.4)$$

The residual field is downward continued and a correction to the surface density of the mass. The correction affects the undulating amplitude of the density boundary. This procedure is repeated iteratively, obtaining at each iteration step  $k$  the residual gravity field  $\delta g_k(x, y)$  and the oscillating amplitude of the boundary  $r_k(x, y)$ . The iterations are repeated until the root mean square (short: RMS) gravity residual achieves an acceptable value or until the successive iteration does not give a considerable enhancement to the results.

This procedure was applied in the area of Pacific Ocean (see chapter 3.1). Thereby seismic data regarding the depth of the studied boundary was integrated into the inversion procedure. A set of inversions was carried out for the different values of the reference depth and the density contrast.

### 1.3.3 Synthetic example

The inversion method was tested on a synthetic model by BRAITENBERG & ZADRO (1999), to investigate the behavior of the solution and the significance of the input parameter. Gaussian noise has been added to the synthetic gravity field. The model has the shape of two rectangular prism set on the top of each other. The upper prism lay in the depth of  $8km$ , with

20km width, 30km length and 1km height. The lower prism is directly under the first one in 9km depth, with 10km width, 10km length and 1km height. The density contrast was set to  $\Delta\rho = -400\text{kg}/\text{m}^3$ . The constraining values for the CMI are used to find an adequate density contrast and boundary reference depth (see Table 1.3.1). For every couple of density contrast and reference depth a test inversion with six iteration steps has been made (BRAITENBERG & ZADRO 1999).

		Reference depth [km]						
		4	6	8	10	12	14	16
Density contrast [ $\text{kg}/\text{m}^3$ ]	-200	3.9	1.7	1.3	3.9	7.2	11.4	16.9
	-300	4.3	2.1	0.5	2.7	5.3	8.5	12.4
	-400	4.4	2.3	0.3	2.2	4.6	7.4	10.6
	-500	4.5	2.4	0.4	1.9	4.2	6.8	9.7
	-600	4.6	2.5	0.5	1.8	4.0	6.4	9.1

**Table 1.3.1)** The root mean square deviation (short: RMS) of the inverted root from the given synthetic CMI was calculated for different couples of reference depth and density contrast. The blue marked cell represents the couple for minimal RMS value which coincident with the input data.

These results lead to three conclusions. First, the best fitting couple is equivalent to the given input data (blue marked cell in Table 1.3.1), as for the couple with reference depth  $d = 8\text{km}$  and density contrast  $\Delta\rho = -400\text{kg}/\text{m}^3$  the minimal RMS value is obtained. Therefore the error made due to the approach can be estimated. The Parker algorithm gives a RMS value of 0.3. The second conclusion is the meaning of the reference depth. The reference depth is the depth, where the less dense material of the crust begins to dip into the mantle. The third consequence is that the reference depth has to be chosen carefully. It should be, if possible, constrained by independent results (e.g. seismic data). It is more forgivable to take a “wrong” density contrast than to take a “wrong” reference depth. If no constrains are available, then it is necessary to quantify the error. For an inaccuracy in the depth of  $d = \pm 4\text{km}$  the RMS value  $\leq 5$  is obtained (assuming to use the correct density contrast). In the worst case, for an inaccuracy of  $\Delta\rho = \pm 200\text{kg}/\text{m}^3$  in the density contrast and  $d = \pm 4\text{km}$  in the reference depth an RMS value of 7.2 is estimated.

Therefore it is necessary to use the CMI estimates from other investigations (e.g. seismic data, IGMAS modeling) as constraints for the choice of the two relevant parameters reference depth  $d$  and density contrast  $\Delta\rho$ .

## 1.4 INTERNAL LOADS

Except of topographic loads exist also loads within the elastic lithospheric plate. These loads are called “internal loads”, which have an important influence on the flexure. Both mass deficits and mass surplus increase or decrease the effect of the topographic loads compared with a homogeneous elastic plate. The internal loads are for example mafic intrusions, thermally induced density anomalies variations within the crust. Furthermore the internal loads are caused by variation in composition, e.g. long stretched sediment basins.

### 1.4.1 Calculation of gravity effect of sediments with slice program

Not only the crust mantle interface, but large expanded sediment basins produce also a long-wavelength gravity signal. This has a important influence on the calculation of the CMI depth variation. Accordingly it is necessary to determine the gravity effect of the sediment basin and subtract this effect from the gravity signal.

gravity effect for each layer calculated with Parker algorithm

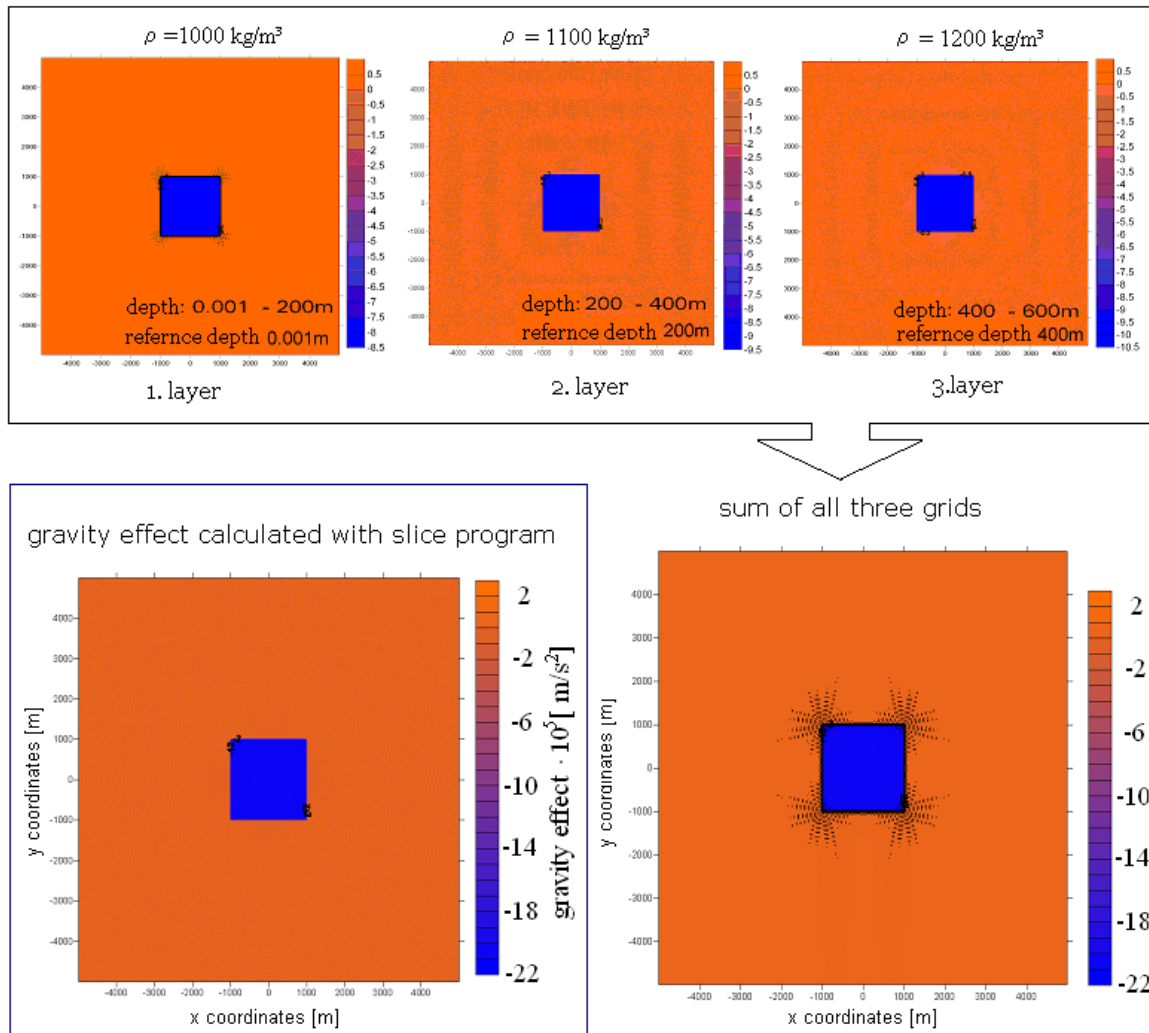


**Figure 1.4.1)** The gravity effect from each layer was calculated according to the Parker algorithm. As evidence for correct calculation of the slice program, the sum of the three gravity grids are taken and compared with the gravity output grid of the slice program. The gravity values of the two grids are in the same domain.



Therefore the software called “slice program” was written by BRAITENBERG (PERS. COMM.), which calculates the gravity effect of a sediment basin. It requires as input parameter the thickness of the sediments. The sediments are divided into slices and per slice one density is taken and the gravity effect is calculated. The calculation is investigated on a synthetic model in order to verify the slice program. The model is a rectangular body which consist of 3 layers:

1. layer: depth  $d = 0.001 - 200m$  and density  $\rho = 1000kg / m^3$
2. layer: depth  $d = 200 - 400m$  and density  $\rho = 1100kg / m^3$
3. layer: depth  $d = 400 - 600m$  and density  $\rho = 1200kg / m^3$

From the whole synthetic body the gravity effect was estimated with the slice program. In a next step from each layer the gravity effect was calculated according to the Parker algorithm. Then the sum of the gravity effect was computed from all three grids. The output grid was compared with the gravity grid calculated with the slice program (Fig. 1.4.1), the same results of the gravity values are obtained. Accordingly, the slice program calculates correctly the gravity effect of the sediments. Additionally, the software was tested with other input shapes (e.g. basin shapes). After verification the slice program was used to compute the gravity effect of the sediments in the area of the Pacific Ocean (see Chapter 3.1). This concept of calculation of the loads of the sediments was used as well by BRAITENBERG ET AL. (2005).

### 1.4.2 Pseudo topography

This concept was developed by GÖTZE & SCHMIDT (PERS. COMM.) in a discussion how to include the internal loads in the estimation of elastic thickness/flexural rigidity. The distribution of the internal loads is usually relatively unknown. The consideration of the internal loads is possible with use of a density model, which represents the material density distribution in the lithosphere. The IGMAS software permits the computation of these internal loads from the density models. Within vertical columns the densities  $\rho_i \quad \forall i = 1, 2, 3 \dots n$  are added successively. If one defined a normal crust density  $\rho_c$  (e.g.  $\rho_c = 2670kg / m^3$ ), one can determine the abnormal load distribution of the lithosphere (Fig. 1.4.2). Together with the topographic load  $h_T \rho_T$  results the entire load  $L_{sum}$  of the plate in one point (PERS. COMM. GÖTZE).

$$L_{sum} = h_T \rho_T + \sum_{i=1}^n h_i \rho_i \quad (1.4.1)$$

The topographic and internal loads are both involved into the Convolution method for calculation of the elastic thickness (see Chapter 3.2 and 3.3). Therefore the internal loads known from the density model are converted into a compensated topography (EBBING ET AL.

2001). This compensated topography here referred to as pseudo topography  $h_{PT}$  contains all abnormal loads of the crust (Fig. 1.4.2).

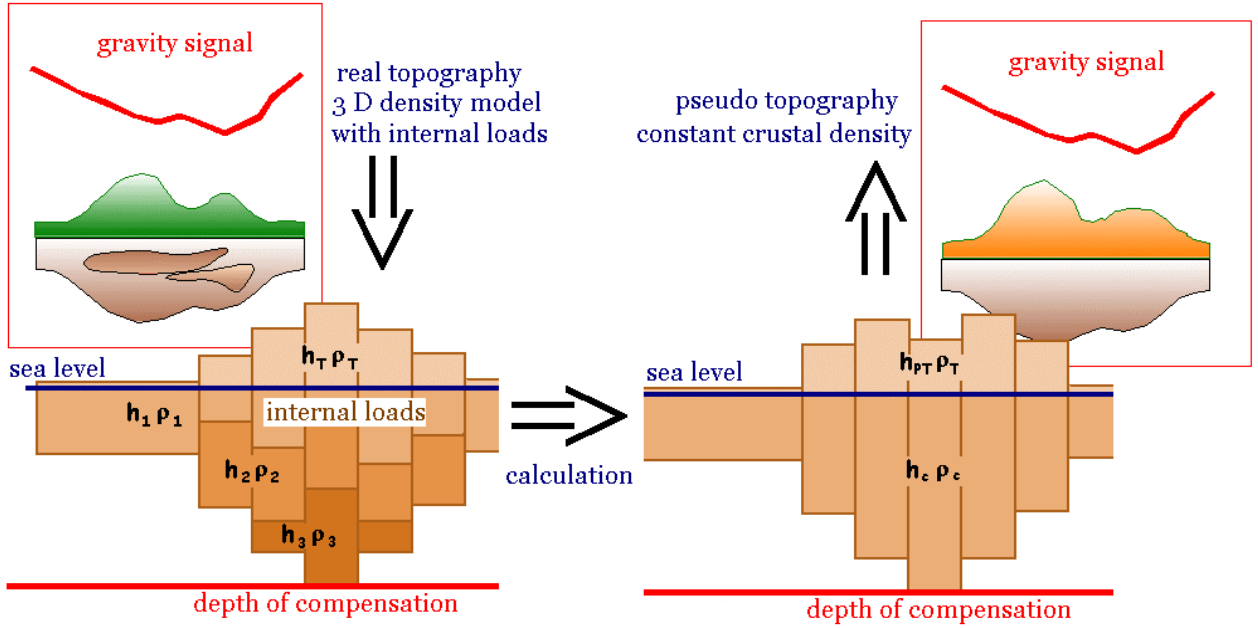


**Figure 1.4.2)** The load acting on the compensation surface (CMI) in the real density model left is just as large as in the model of pseudo topography on the right side. The masses inhomogeneities within the crust are added to the topography, in a way that the crust become homogeneous.

Accordingly the associated plate of the lithosphere can be regarded as homogeneous (PERS. COMM. GÖTZE & EBBING):

$$L_{pseudo} = h_{PT} \rho_T + \sum_{i=1}^n h_i \rho_c = h_{PT} \rho_T + h_c \rho_c \quad (1.4.2)$$

The load acting on the compensation surface in the density model is as large as in the model of pseudo topography. Therefore it is essential that  $L_{pseudo} = L_{sum}$ , which results:

$$h_{PT} \rho_T + h_c \rho_c = h_T \rho_T + \sum_{i=1}^n h_i \rho_i \quad (1.4.3)$$

it follows:

$$h_{PT} = h_T + \frac{\sum_{i=1}^n h_i \rho_i - h_c \rho_c}{\rho_T} \quad (1.4.4)$$

With this formula it is possible to handle the masses inhomogeneities within the crust. The internal loads are added to the topography, in a way that the crust becomes homogeneous. Whereby the load acting at the compensation surface (e.g. CMI) remains constant. Furthermore a constant density contrast at the CMI is assumed (PERS. COMM. GÖTZE).